

Short-Range Ordering of Vacancies in TiO at 1323 K

BY H. TERAUCHI* AND J. B. COHEN

Department of Materials Science & Engineering, The Technological Institute, Northwestern University, Evanston, IL 60201, USA

(Received 17 November 1978; accepted 5 March 1979)

Abstract

The diffuse X-ray scattering from a single crystal of disordered TiO was measured at 1323 K in a volume in reciprocal space. The short-range order parameters between vacancies and cations and anions were determined by Williams's [(1972). Report ORNL-5140. Oak Ridge National Laboratory, Tennessee] least-squares procedure for fitting the total intensity to contributions from this local order and up to quadratic terms in the atomic displacements. Computer simulations with the short-range order coefficients reveal that the local atomic arrangements are similar to those in the low temperature phase. The relationship between this local order and the electronic conductivity is discussed.

Introduction

The monoxides of the first transition series have average structures based on the NaCl arrangement, *Strukturbericht* type B1. However, there are wide ranges in composition and complex point defect arrays including, in some cases, the occupation of interstitial sites by cations (Hayakawa, Morinaga & Cohen, 1973). For TiO ~ 15% of both the anion and cation sites are vacant (Banus & Reed, 1970; Taylor & Doyle, 1970).

Watanabe, Castles, Jostsons & Malin (1967) and Watanabe, Terasaki, Jostsons & Castles (1968, 1970) report that these vacancies in TiO are ordered below 1223 K with a monoclinic structure, *B2/m* (No. 12). We have reported on the detailed structure of the ordered phase (Terauchi, Cohen & Reed, 1978). There are waves of Ti and O ion vacancies every third (110) plane of the pseudocubic unit cell, and no tetrahedrally coordinated interstitial Ti ions could be detected. Castles, Cowley & Spargo (1971) first examined the diffuse intensity with electron diffraction from quenched specimens of the disordered phase; they showed that there was a strong correlation between some of this scattering and the Fermi surface, which was corroborated by Terauchi & Cohen (1978). In the latter study, it was shown that the total diffuse intensity

also implies long-range vacancy–vacancy and vacancy–electron interactions.

In this paper we report on absolute measurements of this diffuse intensity with X-rays to explore the nature of the local vacancy arrangements and their relationship to the ordered phase. The interaction of this local order and the electronic properties of this oxide is discussed.

Experimental procedures

Crystals were grown under a high-purity argon atmosphere, in a tri-arc furnace (Reed & Pollard, 1968) from 99.9% pure TiO₂ and 99.99% pure Ti. Coarse-grained specimens were obtained, with crystals 1 × 1 × 9 mm. After homogenizing at 1473 K for 2 d (in purified argon), one such grain with composition TiO_{0.997} was isolated and polished mechanically; see Banus & Reed (1970) and Terauchi & Cohen (1978) for the method of determining composition.

The X-ray measurements were made on a modified GE XRD-5 diffractometer with a quarter-circle attachment on which was mounted a high temperature furnace with a thin Be hemispherical window for the X-ray beam (Schwartz, Morrison & Cohen, 1964; Gehlen, 1969). Cu K α radiation was obtained from a pyrolytic graphite monochromator in the point-focus incident beam; it was singly bent to focus the beam in a vertical direction (perpendicular to the diffractometer) at the receiving slits. Balanced Ni and Co filters were employed at the detector. Counts were obtained *vs* a fixed number of counts (620 000 in ~10 min) in a monitor detector, which recorded the fluorescence from a thin film of powdered CoO in the exit beam from the monochromator; this minimized the effect of generator instabilities and changes in barometric pressure. The power of the direct beam (~1.9 × 10⁷ Hz at 30 kV, 27 mA) was determined from the integrated intensities of the first four peaks from an Al powder compact (Batterman, DeMarco & Weiss, 1961).

Measurements were made at 1323 ± 2.5 K in an atmosphere of flowing high-purity helium further purified by passing it over Ti chips at 923 K and then through a dry ice trap. Typical counts with the Ni filter

* On leave from Kwansai Gakuin University, Nishinomiya, Japan.

were 1400–4000. Background was determined with a Pb trap in place of the specimen. Ti fluorescence *vs* 2θ was measured with a solid-state detector, and was employed to correct the data for surface roughness (de Wolff, 1956; Suortti, 1972). This measurement also revealed that there was negligible scattering from impurities.

The volume of measurement is shown in Fig. 1; 916 points were obtained in intervals of 0.1 of the reciprocal axes. The intensity at several points and at Bragg peaks was checked periodically and did not change more than 2–3% throughout the entire measurement.

A portion of the observed diffuse intensity is shown in Fig. 2. The diffuse maximum at $\frac{2}{3}, 2, 0$, which we had observed at 1288 K and attributed to long-range vacancy–vacancy interactions out to the sixth neighbor shell (Terauchi & Cohen, 1978), was not found at 1323 K.

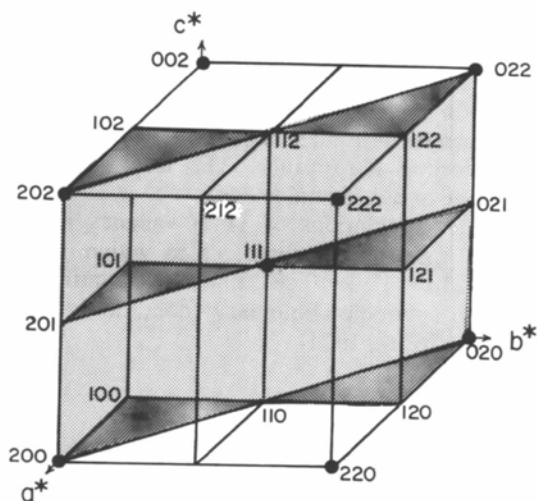


Fig. 1. Measured volume in reciprocal space (shaded).

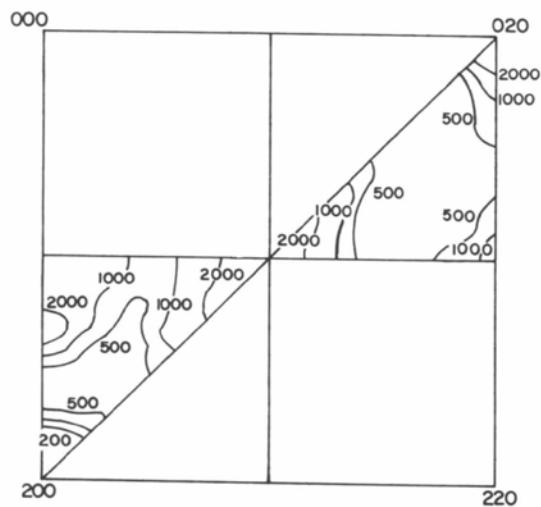


Fig. 2. Observed diffuse intensity at 1323 K; raw intensity in counts, Ni minus Co filter.

Analysis

The diffuse intensity I_0 (in absolute units) includes contributions from local order (I_{SRO}) of the vacancies and from local static and thermal displacements of atoms from the average structure (Hayakawa & Cohen, 1975):

$$I_0 = N(x_O^{\text{Ti}} x_O^{\text{Ti}} f_{\text{Ti}}^2 + x_F^{\text{O}} x_F^{\text{O}} f_{\text{O}}^2)(I_{\text{SRO}} + I_1^{\text{SE}} + I_2^{\text{SE}}). \quad (1)$$

Here, N is the number of lattice points under the X-ray beam, x_O^{Ti} and x_O^{Ti} are the fractions of Ti cations and vacancies on the octahedrally coordinated cation sublattice (O) and correspondingly for the oxygen ions on the face-centered cubic sublattice (F), x_F^{O} , x_F^{O} are the respective sublattice fractions; the f_i are the scattering factors. These were taken from *International Tables for X-ray Crystallography* (1974) and corrected for the individual temperature factors measured at room temperature (Terauchi & Cohen, 1978). I_1^{SE} is due to mean static displacements, and I_2^{SE} is quadratic in the static and dynamic displacements. The first term in parentheses is the (Laue) monotonic scattering (I_{LM}) per structural unit.

Each term in (1) can be written as a series in terms of the reciprocal space coordinates h_1, h_2, h_3 ;

$$I_{\text{SRO}}(h_1, h_2, h_3) = \sum_{l,m,n} \bar{\alpha}_{lmn} \cos 2\pi(h_1 l + h_2 m + h_3 n), \quad (2a)$$

where the lmn define an average interatomic vector,

$$\mathbf{r}_{lmn} = l \frac{\mathbf{a}}{2} + m \frac{\mathbf{b}}{2} + n \frac{\mathbf{c}}{2}. \quad (2b)$$

There are two types of interatomic vectors in this structure which can be distinguished in terms of integers p and q :

$$\left. \begin{aligned} l, m, n &= 2p/4 \\ l + m + n &= 4q/4 \end{aligned} \right\} \begin{array}{l} \text{f.c.c.} - \text{f.c.c., octahedral} \\ \text{sites} - \text{octahedral,} \end{array} \quad (3a)$$

$$\left. \begin{aligned} l, m, n &= 2p/4 \\ l + m + n &= (4q + 2)/4 \end{aligned} \right\} \text{f.c.c.} - \text{octahedral sites.} \quad (3b)$$

For type 1 vectors (Hayakawa & Cohen, 1975):

$$\bar{\alpha}_{lmn} = \frac{x_F^{\text{O}} x_F^{\text{O}} f_{\text{O}}^2 \alpha_{\text{FF}}^{\text{O}} + [x_O^{\text{Ti}} x_O^{\text{Ti}} f_{\text{Ti}}^2 \alpha_{\text{OO}}^{\text{Ti}}(lmn)]}{x_F^{\text{O}} x_F^{\text{O}} f_{\text{O}}^2 + x_O^{\text{Ti}} x_O^{\text{Ti}} f_{\text{Ti}}^2}, \quad (4a)$$

and for type 2 vectors:

$$\bar{\alpha}_{lmn} = \frac{2f_{\text{O}} f_{\text{Ti}} x_O^{\text{Ti}} x_F^{\text{O}} \alpha_{\text{OF}}^{\text{Ti}}(lmn)}{x_F^{\text{O}} x_F^{\text{O}} f_{\text{O}}^2 + x_O^{\text{Ti}} x_O^{\text{Ti}} f_{\text{Ti}}^2}. \quad (4b)$$

Here, for example:

$$\alpha_{OO}^{TiV_{Ti}}(lmn) \equiv 1 - \frac{P_{OO}^{TiV_{Ti}}}{x_O^{V_{Ti}}}(lmn), \quad (5)$$

where $P_{OO}^{TiV_{Ti}}$ is the conditional probability of finding a vacancy on the cation sublattice in the octahedral sites of the oxygen f.c.c. sublattice at the end of vector \mathbf{r}_{lmn} if there is a cation at the origin of the vector.

For type 2 vectors, only one local order parameter (α) is involved, but for type 1 vectors there are two. From the condition on P_{uv}^{ij} that

$$0 \leq P_{uv}^{ij} \leq 1, \quad (6)$$

we get:

$$-0.702 = -(x_F^O)^2 \leq x_F^O x_F^{V_O} \alpha_{FF}^{O_{FF}^O} \leq x_F^O x_F^{V_O} = 0.136, \quad (7a)$$

$$-0.707 = -(x_O^{Ti})^2 \leq x_O^{Ti} x_O^{V_{Ti}} \alpha_{OO}^{TiV_{Ti}} \leq x_O^{Ti} x_O^{V_{Ti}} = 0.134. \quad (7b)$$

The diffuse scattering measurements were made in the range $\sin \theta/\lambda = 0.15-0.45$. Hence,

$$0.500 \leq f_O^2/I_{LM} \leq 0.887 \quad (8a)$$

(where I_{LM} is the denominator of equations 4),

$$6.578 \leq f_{Ti}^2/I_{LM} \leq 6.970. \quad (8b)$$

Employing values at the center of the measuring range (the result is not seriously affected by this choice);

$$\bar{\alpha}_{lmn} = 0.089 \alpha_{FF}^{O_{FF}^O}(lmn) + 0.911 \alpha_{OO}^{TiV_{Ti}}(lmn). \quad (9a)$$

In the ordered phase, the waves of titanium vacancies have twice the amplitude as those for the oxygen ion vacancies and therefore it seems likely that $\alpha_{OO}^{TiV_{Ti}} \geq \alpha_{FF}^{O_{FF}^O}$. Therefore $\bar{\alpha}_{lmn} \simeq \alpha_{OO}^{TiV_{Ti}}(lmn)$.

Again, employing values at the center of the measuring range for type 2 vectors:

$$\alpha_{OF}^{TiV_{Ti}}(lmn) = 1.74 \bar{\alpha}_{lmn}. \quad (9b)$$

Thus it is possible in this complex situation to obtain some information on the local order between Ti ions and vacancies and between Ti ions and oxygen vacancies; the local order between oxygen ions and oxygen vacancies cannot be examined separately.

The displacement terms are correspondingly complex:

$$I_1^{SE} = \sum_j \sum_{lmn} \bar{\gamma}^j(lmn) h_j \sin 2\pi(h_1 l + h_2 m + h_3 n), \quad (10)$$

$$I_2^{SE} = \sum_j \sum_{lmn} \bar{\delta}^j(lmn) h_j^2 \cos 2\pi(h_1 l + h_2 m + h_3 n) \\ + \sum_j \sum_{lmn} \bar{\epsilon}^{j,j+1}(lmn) h_j h_{j+1} \\ \times \cos 2\pi(h_1 l + h_2 m + h_3 n). \quad (11)$$

Unfortunately, $\bar{\gamma}$, $\bar{\delta}$, $\bar{\epsilon}$ involve α_{FF} ; the weighting of the various α 's is not sufficient to minimize this contribution. Each of these coefficients are complex sums of the displacements of the various types of pairs which cannot be separated. Accordingly we will make only qualitative comments on these terms, and there is no point in providing the detailed equations. (These can be readily obtained from the procedures described in Hayakawa & Cohen, 1975.)

After correcting the raw data from the two filters for surface roughness and parasitic scattering, these were placed on an absolute scale, calculated Compton scattering was subtracted (*International Tables for X-ray Crystallography*, 1962) and the $\bar{\alpha}$, $\bar{\gamma}$, $\bar{\delta}$, $\bar{\epsilon}$ were obtained by a least-squares fit to the total remaining intensity (Williams, 1972). This method is quite sensitive to the regions in reciprocal space that are included and to the number of displacement terms (Morinaga, 1978) and these must be monitored. In this oxide, the minimum volume in reciprocal space required to separate the intensity terms by symmetry (Borie & Sparks, 1971) and then to perform a Fourier inversion for the coefficients, is so large as to preclude its measurement in a reasonable time with the intensity from a normal X-ray tube. The least-squares procedure is the only reasonable one.

Computer simulations of Ti-Ti vacancy arrays to satisfy the first six measured α 's to within 1% were made with $10 \times 10 \times 10$ cells of the Ti sublattice (4000 sites) with periodic boundary conditions (Gragg, Bardhan & Cohen, 1971).

Results and discussion

There were no strong correlations between the coefficients in the least-squares fit to the intensity. The separated I_{SRO} is plotted in Fig. 3. Some 13 data points

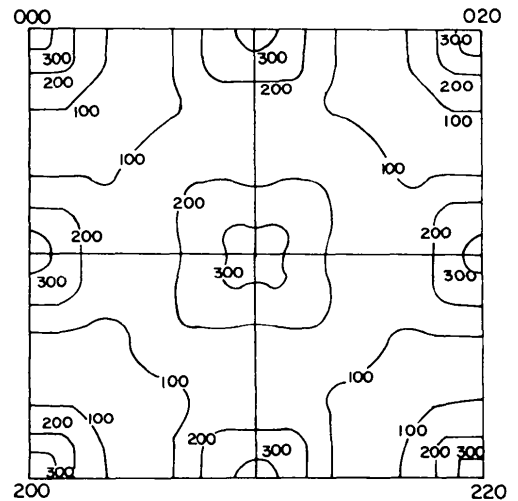


Fig. 3. Separated I_{SRO} , Laue units per atom.

near Bragg peaks were removed and 30 others were smoothed prior to the least-squares fit. The stability of this fit was examined by adding terms, and the most stable solution with $\alpha_{000} \approx 1$ was chosen. The resulting coefficients are given in Table 1 and the α_{lmn} are plotted for both types of vectors in Fig. 4. The reliability index, R , defined as

$$R = \left[\frac{\sum_{i=1}^n w_i (I_{\text{obs}}^{i/2} - I_{\text{calc}}^{i/2})^2}{\sum_{i=1}^n w_i I_{\text{obs}}^i} \right]^{1/2}, \quad (12a)$$

$$w_i = I_{\text{obs}}^i, \quad (12b)$$

was 23%.

Sauvage & Parthé (1974) have suggested that the local order in defect oxides (or solid solution oxides) might follow Pauling's electrostatic valency rules, and that the overall composition would be satisfied on the smallest structural unit. There are several objections to applying this concept to TiO. In the first place, it is metallic, not ionic and there is evidence for long-range interactions (Terauchi & Cohen, 1978). Secondly, there are cation *and* anion vacancies. One might assume that octahedra around both species follow this rule and that there is little interaction. In such a case, we might consider for example two types of Ti octahedra, one containing four Ti ions and two vacancies and one containing six Ti atoms and no vacancies. The latter might occur around an oxygen ion, the former around a partially ionized oxygen vacancy. Applying Sauvage & Parthé's equations, 45% of the octahedra would

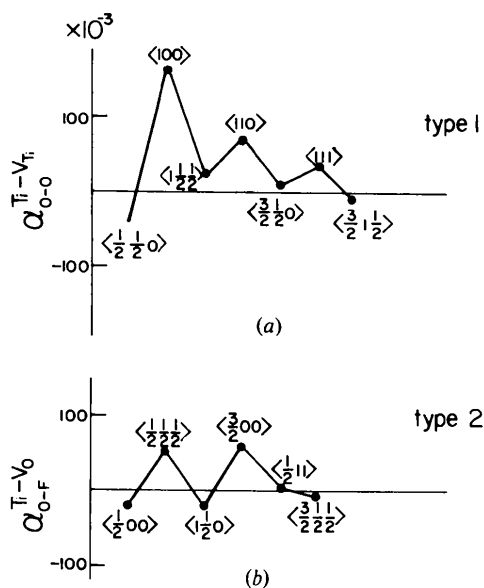


Fig. 4. Short-range order parameters, for Type 1 (a) and Type 2 (b) interatomic vectors.

contain the two vacancies and then, again following these authors:

$$(\cos \pi h_1 + \cos \pi h_2 + \cos \pi h_3)^2 = 0.32 = \alpha_0^{\text{TiV}^{\text{Ti}}} + 4\alpha_1^{\text{TiV}^{\text{Ti}}} + \alpha_2^{\text{TiV}^{\text{Ti}}}. \quad (13)$$

The measured α 's sum to 1.09, and thus this approach is not valid in this material. (Other types of octahedra were considered, but these did not improve the comparison.)

Sections of the ordered phase of TiO on (001), (110) and (120) planes are shown in Fig. 5. (Only the Ti ions and vacancies are shown.) The same planes were examined quantitatively in the computer simulations with the measured α 's, and in a simulation where $\alpha_1 - \alpha_6 = 0$, *i.e.* a near-random Ti-Ti vacancy sublattice, looking for the obvious features in Fig. 5. For example, the parallelograms in Fig. 5(a) were sought, with corners occupied by three or four vacancies, rather than the four in the ordered phase. Regions similar to those in Fig. 5(b) can be seen in the simulations in Figs. 6(a) and (b), and the vacancy clusters along [001] directions in Fig. 5(b) are shown in the simulations in Figs. 6(c) and 6(d). These were counted, as well as the vacancy clusters on (120) planes shown in Fig. 5(c). The results are presented in Table 2. The tendency for regions like the ordered state is clear but the periodic

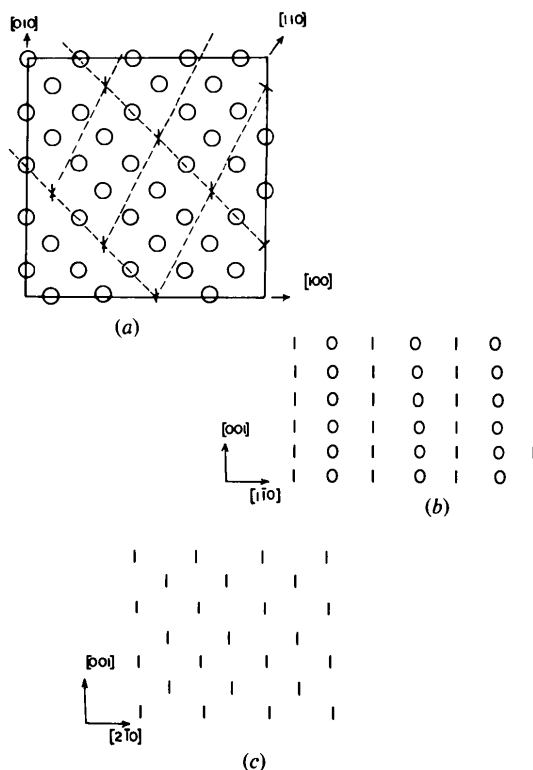


Fig. 5. Some planes in ordered TiO. 1 = vacancy, 0 = cation (Ti sublattice only). (a) (001) plane. (b) Every third (110) plane. (c) Every sixth (120) plane.

Table 1. *The coefficients of the total diffuse intensity*

Type 1 vectors										
2(lmn)	$\alpha_{00}^{TiTi}(lmn)$	$\gamma^x(lmn)$	$\gamma^y(lmn)$	$\gamma^z(lmn)$	$\delta^{xx}(lmn)$	$\delta^{yy}(lmn)$	$\delta^{zz}(lmn)$	$\epsilon^{xy}(lmn)$	$\epsilon^{yz}(lmn)$	$\epsilon^{zx}(lmn)$
000	1.0895	0	0	0	0.0099	0.0099	0.0099	0	0	0
110	-0.0409	0.0017	0.0017	0.0000	0.0067	0.0066	0.0066	0.0113	0.0000	0.0000
200	0.1736	0.0024	0.0000	0.0000	0.0203	0.0171	0.0171			
211	0.0195	-0.0234	0.0132	0.0132	0.0028	0.0006	0.0006			
220	0.0792	-0.0131	-0.0131	0.0000						
310	0.0093	-0.0100	-0.0249	0.0000						
222	0.0452	-0.0033	-0.0033	-0.0033						
321	-0.0035									

Type 2 vectors	
2(lmn)	$\alpha_{0F}^{TiO}(lmn)$
100	-0.0360
111	0.0990
210	-0.0398
300	0.1087
122	0.0163
311	-0.0261

variation in the vacancy concentration in a $\langle 110 \rangle$ direction found in the ordered phase, was not present. Other kinds of regions were sought; for example in VO_x (Morinaga, 1978), there are vacancy rich (111) planes, but no excess number of these over the random simulation could be found in the simulation with the measured α 's for TiO.

The numbers of various Ti-Ti-vacancy triplets and quadruplets are given in Table 3. In the ordered phase, a Ti vacancy is surrounded by 12 Ti ions. In the locally ordered state, note the excess of triplets and quadruplets involving one vacancy.

The distribution of Ti vacancies in shells around such a vacancy is examined further in Fig. 7. These distributions differ from those in the near-random simulation only in the second and fourth shells.

The (negative) value for $\alpha_{0F}^{TiO}(\frac{1}{2}00)$ and $\alpha_{00}^{TiTi}(\frac{1}{2}, \frac{1}{2}, 0)$ implies that a Ti ion tends to surround itself with vacancies on *both sublattices*.

The larger γ terms in Table 1 are negative suggesting a collapse of the ions towards a vacancy. But it is curious that this occurs in distant shells, *not* at the nearest neighbors. Furthermore, these displacement terms do not follow the oscillations of the short-range order parameters.

While TiO is metallic its resistivity is high ($\sim 10^{-5}$ Ω m, Banus & Reed, 1970). Goodenough (1972) has suggested that the splitting of the t_{2g} band and its narrowness could explain this behavior; the band width and electron correlation energy must be similar in magnitude in this material. However there may be an important contribution to the band structure from the local vacancy order (Lifshitz, 1964). Following treatments for liquid metals, the resistivity (ρ) may be written (Ziman, 1970)

$$\rho \propto |U_{2k_F}|^2 \alpha_{q=2k_F} \quad (14)$$

Table 2. *Quantitative analysis of computer simulations of Ti sublattice*

(001) planes		
Sizes of parallelogram-like regions on (001) planes. See Fig. 5(a).	Number of regions	
	Random	SRO
1	74	78
2	2	6
3	0	1
4	0	0

(110) planes		
Size of regions. (a) See Figs. 5(b), 6(b).	Number of regions	
	Random	SRO
1	50	56
2	8	16
3	1	8
4	0	2
5	0	0
6	0	1

(b) See Figs. 5(b), 6(c), (d).	Number of clusters	
	Random	SRO
1 vacancy isolated from others	469	309
2 vacancies clustered along [001]	60	93
3	13	33
4	2	5
5	0	3
6	0	0
7	0	1

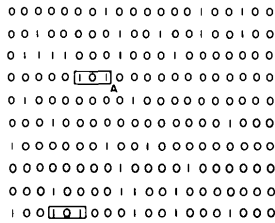
(120) planes		
Vacancy cluster size (see Fig. 5c).	Number of clusters	
	Random	SRO
2 vacancies	57	56
3 vacancies	35	37
4 vacancies	13	16
5 vacancies	8	13
6 vacancies	2	6
7 vacancies	4	2
8 vacancies	0	5
9 vacancies	0	2
10 vacancies	0	0
11 vacancies	0	1

Here, U_q is the Fourier transform of a (screened) pseudopotential and $\alpha_q \equiv I_{\text{SRO}}(h_i)$ is a measure of the Fermi surface in momentum (q) space (Morinaga, 1977). The term $2k_F$ is the caliper of the Fermi distribution. This equation merely states that the largest

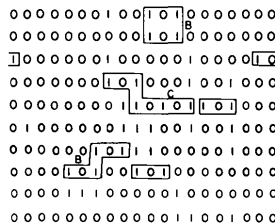
contribution to the resistivity should come from electrons that can suffer momentum changes that span the Fermi distribution, *i.e.* from the electrons near the Fermi surface. Now U_q is slowly varying (Shaw, 1968) and the I_{SRO} is large in both the $\langle 100 \rangle$ and $\langle 110 \rangle$ directions at exactly this $2k_F$ position in reciprocal space (see also Castles, Cowley & Spargo, 1971; Terauchi & Cohen, 1978). Therefore a significant contribution by the local order to the resistivity is possible in this system.

Table 3. Near-neighbor triplets and quadruplets on the Ti sublattice in computer simulations

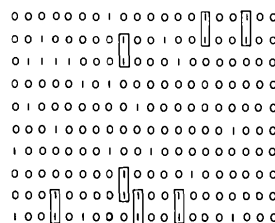
Number of triplets	Random	SRO
Ti-Ti-Ti	19032	18547
Ti-Ti-V _{Ti}	10804	11735
Ti-V _{Ti} -V _{Ti}	2032	1625
V _{Ti} -V _{Ti} -V _{Ti}	132	93
Number of quadruplets		
Ti-Ti-Ti-Ti	3998	3775
Ti-Ti-Ti-V _{Ti}	3040	3447
Ti-Ti-V _{Ti} -V _{Ti}	842	697
Ti-V _{Ti} -V _{Ti} -V _{Ti}	116	77



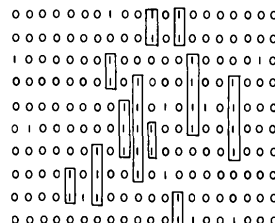
(a) Random



(b) S.R.O.



(c) Random



(d) S.R.O.

Fig. 6. Typical $\langle 110 \rangle$ sections from computer simulations. A = size 1, B = size 2, C = size 3 in Table 2 (Ti sublattice only).

Further studies of the role of local order on conductivity in these oxides is underway with VO_x (Morinaga, 1978); by adjusting the composition, x , the conductivity can be changed from metallic to semi-conducting (Banus & Reed, 1970). It will be interesting to see if and how the local defect structure changes.

The authors thank Dr T. B. Reed, (formerly at Lincoln Laboratories) for supplying the crystals, Mr C. Tang for his detailed analysis of the complete simulations, Messrs R. Comstock, W. Schlosberg, J. Georgopoulos and especially Dr M. Morinaga for advice and assistance.

The use of the long-term X-ray facility of Northwestern University's Materials Research Center, supported in part under the NSF-MRL program (grant

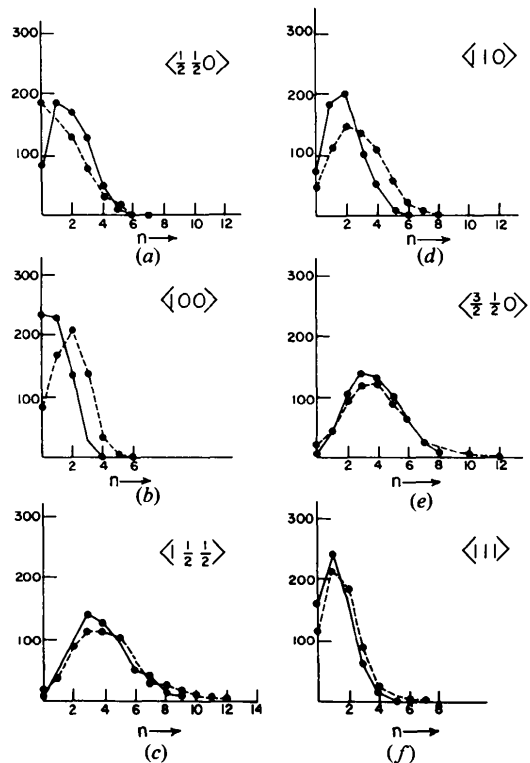


Fig. 7. Number of Ti vacancies having n Ti vacancies as neighbors in the indicated shell, from computer simulations. — SRO, ---- near-random.

DMR-76-80847) facilitated this work. The research was supported by the US Army Research Office under grant No. DAAG29-78-G-0156.

References

- BANUS, M. D. & REED, T. B. (1970). *The Chemistry of Extended Defects in Non-Metallic Solids*, edited by L. EYRING & M. O'KEEFE, pp. 488–522. Amsterdam: North-Holland.
- BATTERMAN, B. W., DEMARCO, J. J. & WEISS, R. J. (1961). *Phys. Rev.* **122**, 68–74.
- BORIE, B. & SPARKS, C. J. (1971). *Acta Cryst.* **A27**, 198–201.
- CASTLES, J. R., COWLEY, J. M. & SPARGO, A. E. C. (1971). *Acta Cryst.* **A27**, 376–383.
- GEHLEN, P. C. (1969). *Rev. Sci. Instrum.* **40**, 718–721.
- GOODENOUGH, J. B. (1972). *Phys. Rev. B*, **5**, 2764–2774.
- GRAGG, J. E. JR, BARDHAN, P. & COHEN, J. B. (1971). *Critical Phenomena in Alloys, Magnets and Superconductors*, edited by R. E. MILLS, E. ASCHER & R. I. JAFFEE, pp. 309–337. New York: McGraw-Hill.
- HAYAKAWA, M. & COHEN, J. B. (1975). *Acta Cryst.* **A31**, 635–644.
- HAYAKAWA, M., MORINAGA, M. & COHEN, J. B. (1973). *Defects and Transport in Oxides*, edited by M. S. SELTZER & R. I. JAFFEE, pp. 177–199. New York: Plenum Press.
- International Tables for X-ray Crystallography* (1962). Vol. III. Birmingham: Kynoch Press.
- International Tables for X-ray Crystallography* (1974). Vol. IV. Birmingham: Kynoch Press.
- LIFSHITZ, I. M. (1964). *Adv. Phys.* **13**, 483–536.
- MORINAGA, M. (1977). *Acta Metall.* **25**, 957–962.
- MORINAGA, M. (1978). PhD Thesis, Northwestern Univ., Evanston, IL 60201.
- REED, T. B. & POLLARD, E. R. (1968). *J. Cryst. Growth*, **2**, 243–247.
- SAUVAGE, M. & PARTHÉ, E. (1974). *Acta Cryst.* **A30**, 239–246.
- SCHWARTZ, L. H., MORRISON, L. H. & COHEN, J. B. (1964). *Adv. X-ray Anal.* **7**, 281–301.
- SHAW, B. W. (1968). *Phys. Rev.* **174**, 769–781.
- SUORTTI, P. (1972). *J. Appl. Cryst.* **5**, 325–331.
- TAYLOR, A. & DOYLE, N. J. (1970). *The Chemistry of Extended Defects in Non-metallic Solids*, edited by L. EYRING & M. O'KEEFE, pp. 523–540. Amsterdam: North-Holland.
- TERAUCHI, H. & COHEN, J. B. (1978). *J. Phys. Chem. Solids*, **39**, 681–686.
- TERAUCHI, H., COHEN, J. B. & REED, T. B. (1978). *Acta Cryst.* **A34**, 556–561.
- WATANABE, D., CASTLES, J. R., JOSTSONS, A. & MALIN, A. (1967). *Acta Cryst.* **23**, 307–313.
- WATANABE, D., TERASAKI, O., JOSTSONS, A. & CASTLES, J. R. (1968). *J. Phys. Soc. Jpn*, **25**, 292.
- WATANABE, D., TERASAKI, O., JOSTSONS, A. & CASTLES, J. R. (1970). *The Chemistry of Extended Defects in Non-Metallic Solids*, edited by L. EYRING & M. O'KEEFE, pp. 238–258. Amsterdam: North-Holland.
- WILLIAMS, R. O. (1972). Report ORNL-5140. Oak Ridge National Laboratory, Tennessee.
- WOLFF, P. M. DE (1956). *Acta Cryst.* **2**, 682–683.
- ZIMAN, J. M. (1970). *Proc. R. Soc. London Ser. A*, **318**, 401–420.

Acta Cryst. (1979). **A35**, 652–658

The Use of Electric Field Gradient Calculations in Charge Density Refinements. I. Hirshfeld-Type Deformation Functions and the Calculation of Electric Field Gradients by Fourier Series

BY D. SCHWARZENBACH AND NGO THONG

Institut de Cristallographie, Université de Lausanne, Bâtiment des Sciences Physiques, 1015 Lausanne, Switzerland

(Received 20 January 1979; accepted 26 February 1979)

Abstract

Single-crystal X-ray diffraction data contain in principle complete information on the spatial distribution of the bonding electrons. However, this information is subject to a variety of errors. Nuclear quadrupole resonance spectroscopy (NQR) provides a very sensitive measurement of an electrostatic property of the deformation density; the electric field gradient tensor at the site of a nucleus. It is proposed that diffraction

and NQR data are combined so that more reliable charge densities can be obtained. Well known multipole deformation functions are used to describe a quasi-static and parametrized deformation density. The electric field gradient is computed by a Fourier series and expressed as a function of the same deformation parameters. These can then be refined by least-squares calculations simultaneously with respect to diffraction intensities and NQR results. Overlap corrections of the neutral spherical atoms and the effect of temperature vibrations are discussed.